Dynamic Structure Factor of Diblock Copolymers Solutions in the Disordered State. 3. The Non-Mean-Field Regime

P. Holmqvist,[†] S. Pispas,[‡] N. Hadjichristidis,*[,‡] G. Fytas,*[,†] and R. Sigel[†,§]

FORTH−Institute of Electronic Structure and Laser, P.O. Box 1527, 71110 Heraklion, Crete, Greece, and Department of Chemistry, University of Athens, 15701 Zografou, Athens, Greece

Received August 29, 2002; Revised Manuscript Received November 21, 2002

ABSTRACT: The dynamic structure factor $S(q,t)$ of seven diblock copolymers in a common solvent was measured by photon correlation spectroscopy as a function of concentration (ϕ) in the disordered state near the disordered-to-order transition (ODT). Both symmetric and asymmetric diblock copolymers of styrene-*b*-isoprene (SI) with molecular masses ranging from 0.95 to 3.6 million g/mol and their hydrogenated styrene-*b*-(ethylene-*alt*-propylene) (SEP) counterparts have been considered. The maximum of the static structure factor $S(q^*)$ and the characteristic spacing $1/q^*$ do not conform to theoretical predictions over the whole ϕ range up to ϕ_{ODT}. The $S(q,t)$ is determined mainly by the relative contribution of two relaxation processes one of which is diffusive (q^2-dependent rate). When composition fluctuation corrections become important for $S(q^*)$ at $\phi_x < \phi_{ODT}$, $S(q,t)$ exhibits a dynamic crossover from a dominant pure relaxational (q-independent rate) to a dominant diffusive character. This new dynamic behavior in the shape of $S(q,t)$ of narrowly distributed diblock copolymer solutions is captured theoretically. Above about ϕ_x, the self-diffusion coefficient $D_s(\phi)$ obtained from the $S(q,t)$ at low q/q^* values becomes thermodynamically retarded. The real phase morphology of diblock copolymers is well complemented by their dynamic structure.

I. Introduction

The dynamic response of diblock copolymer solutions in the homogeneous, mean-field, regime has been thoroughly addressed both experimentally and theoretically.[1−6] As the order−disorder transition (ODT) is approached with increasing diblock copolymer concentration, ϕ, the composition fluctuations, ϕ_q, progressively deviate from those expected from the mean-field static structure factor $S(q) = \langle|\phi_q|\rangle^2$ in particular at wave vectors, **q**, matching the size R of the chain i.e., $q^*R \approx 2$. The understanding of the dynamic response, best investigated nowadays by photon correlation spectroscopy (PCS), relies on the identification of the dominant mechanisms in the relaxation of the order parameter fluctuation, $\phi_q(t)$, manifested in the dynamic structure factor, $S(q,t) = \langle\phi_q(t)\phi_{-q}(0)\rangle$. In the mean-field regime of the disordered phase, there is a consensus on the assignment of the two main relaxation processes in $S(q,t)$ with chain self-diffusion and chain overall motion. Further, it was recently shown[7] that the dominant relaxation process is sensitive to the presence of composition polydispersity, $\langle\delta f^2\rangle$, and can change from a relaxational (q-independent rate) to a diffusive (q^2-dependent rate) character with increasing polydispersity.

This paper addresses the evolution of the dominant process in diblock copolymer solutions in a nonselective solvent with increasing ϕ. The well-documented[8] non-mean-field behavior of $S(q)$ approaching the ODT, in sufficiently monodisperse samples, is accompanied by a dynamic crossover where the dominant process of $S(q,t)$ changes from a relaxational to a diffusive character. This dynamic crossover is captured by the theoretical predictions for polydisperse diblock copolymers.[9] Not only is the evolution of $S(q,t)$ with ϕ of interest but also the ϕ dependence of the diffusion coefficient, D_s, extracted from the $S(q,t)$ at $q < q^*$. The deviation from the predicted concentration dependence of D_s for entangled polymers in a good solvent[10,11] is discussed in terms of an activation energy induced by non-mean-field composition fluctuations approaching the ODT.[12] Finally, the static parameters, q^* and $S(q^*)$, were found to deviate from the scaling proposed theoretically[13,14] for diblock copolymer solutions in a good nonselective solvent where the excluded-volume interactions and composition fluctuations are accounted for.

II. Theoretical Background

A. Monodisperse Systems. The order parameter (composition) fluctuations, $\phi_q(t)$, are manifested in the intermediate scattering function $S(q,t) = \langle\phi_q(t)\phi_{-q}(0)\rangle$. For unentangled (Rouse) block copolymer melts[15,16] and solutions,[1−6] $S(q,t)$ has been treated theoretically using the dynamic random phase approximation (RPA) approach. In the general case of entangled block copolymers[5] and in the frame of the reptation model, the motional mechanisms of both tube-conformation and tube-length fluctuations can relax $\phi_q(t)$. $S(q,t)$ is therefore the sum of the contributions of the reptation, $S^{(rep)}(q,t)$, and Rouse, $S^{(R)}(q,t)$, dynamic structure factors.[5] For pure reptational motion, the scattering function

$$S^{(rep)}(q,t) = \sum_k I_k^{(rep)}(q) \exp(-\Gamma_k^{(rep)}(q)t) \qquad (1)$$

involves a set of relaxation rates $\Gamma_k^{(rep)}(q)$ ($k = 0, 1, 2, ...$) and intensities $I_k^{(rep)}(q)$ evaluated from the susceptibility of the system. The intensity $I_1^{(rep)}$ of the first higher-order mode ($k = 1$) is about 100 times weaker than that of the main ($k = 0$) mode. For $q < q^*$, the

[†] FORTH−Institute of Electronic Structure and Laser.
[‡] University of Athens.
[§] Present address: Max Planck Institute of Colloids and Interfaces, 14476 Golm, Germany .

10.1021/ma021402p CCC: $25.00
Published on Web 01/04/2003

rate $\Gamma_0^{(rep)} \cong 1/\tau_0$ (τ_0 is the longest chain relaxation time) has been verified experimentally.[6] The additional contribution of chain conformation fluctuations inside the tube described by the Rouse model reads:

$$S^{(R)}(q,t) = \sum_j I_j^{(R)}(q) \exp(-tj^2/\tau_R) \qquad (2)$$

From the intensities $I_j^{(R)}(q)$ ($j = 1, 2, 3, ...$) only the stronger $I_1^{(R)}(q)$ and the corresponding Rouse time $\tau_R \propto N^2$ of the first mode appear to be experimentally relevant,[5] where $N = N_A + N_B$ is the total number of links per AB chain. For $q < q^*$ both $I_0^{(rep)}(q)$ and $I_1^{(R)}(q)$ scale with q^2 and the relative contribution of $S^{(rep)}(q,t)$ and $S^{(R)}(q,t)$ to $S(q,t)$ is $I_0^{(rep)}(q)/I_1^{(R)}(q) \cong (24\pi^2)N/N_e$ and $\tau_0/\tau_R = (3\pi^2/4)N/N_e$ with N_e being the number of links between entanglements along the AB chain. A thorough comparison between experimental and theoretical $S(q,t)$ of symmetric and asymmetric high molecular weight styrene−isoprene (SI) entangled diblock copolymer solutions in the common solvent toluene has clearly identified these two relaxation mechanisms in the disordered mean-field regime.[6,7] The mean-field dynamic behavior of AB block copolymer systems at $q \leq q^*$ is purely relaxational since Γ_0 and $\Gamma_R = 1/\tau_R$ are q-independent; the total polymer concentration fluctuations relax via the fast cooperative diffusion as in semidilute solutions of homopolymers.[3,6] Static mean-field behavior is experimentally reflected in the linear dependence of $S(q^*)^{-1}$ vs T^{-1} in the undiluted state or $S(q^*)^{-1}$ vs diblock copolymer concentration, ϕ, at constant temperature, T.

B. Polydisperse Diblock Copolymers. The presence of a finite polydispersity is inevitable in synthetic polymers. For AB block copolymers this inefficiency of the macromolecular chemistry also causes composition polydispersity that is responsible for an incoherent scattering source. The large scale ($q \ll q^*$) behavior of $S(q,t)$ is well documented by an additional diffusive process:[3]

$$S_p(q,t) = S_p \exp(-\Gamma_p(q)t) \qquad (3)$$

with q-independent intensity $S_p = \kappa_0/(1 - 2\kappa_0\chi\phi^{1.6}N)$ and q^2-dependent rate $\Gamma_p = q^2D_s(1 - 2\kappa_0\chi\phi^{1.6}N)$ where D_s is the chain self-diffusion coefficient, ϕ is the volume fraction of the block copolymers and $\kappa_0 = \langle f^2\rangle - \langle f\rangle^2 = \langle \delta f^2\rangle/12$ is the composition polydispersity for an AB block copolymer of average composition, f, in A. The total $S(q,t)$ of real AB diblock copolymers at low magnification, $q \ll q^*$, is predicted and found to be the sum of all the contributions of eqs 1−3 while the pure relaxational contribution of eq 1 is responsible for the peak in $S(q \cong q^*)$.[6] On the basis of recent experimental work, however, the $S(q,t)$ of disordered AB diblock copolymers depends sensitively on the presence of polydispersity (in both molecular mass and composition) also in the vicinity of q^*.[7] The pure relaxational decay (see eq 1) can change to a pure diffusive one (cf. eq 3) which becomes the dominant mechanism for the relaxation of the composition fluctuations with $q \sim q^*$; i.e., it accounts for the peak in $S(q \sim q^*)$. The theory of $S(q,t)$ in section II.A has been extended[9] to compositionally polydisperse entangled AB block copolymers assuming reptation dynamics. $S(q,t)$ has identically the form of eq 1, but now the inclusion of composition polydispersity causes a coupling between pure chain relaxation and chain diffusion. The intensities $I_k(q)$ and the rate $\Gamma_k(q)$ of the kth mode can be calculated from

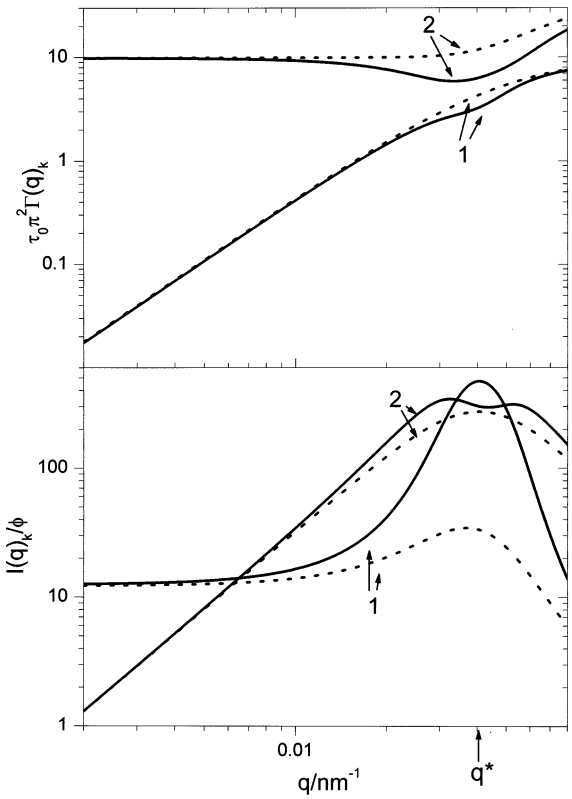

Figure 1. Theoretical predictions for the wave vector, q, dependence of the dimensionless relaxation rates, $\tau_0\pi^2\Gamma_k$, and intensities, I_k, of the first ($k = 1$) and second ($k = 2$) modes (eqs 4 and 5) of the dynamic structure factor, $S(q,t)$, in diblock copolymers using the parameters $\langle \delta f^2\rangle = 0.2$ and $R_g = 50$ nm for $\epsilon = 0.55$ (dashed lines) and $\epsilon = 0.22$ (solid lines). The arrow pointing at the x-axis indicates the q^* at which the total $I(q)$ attains it maximum value.

$$1/\kappa(q,-\Gamma_k) = 0, \quad I_k = \frac{1}{\Gamma_k}\mathrm{Res}_{p=-\Gamma_k}[\kappa(q,p)] \qquad (4)$$

where Res means the residual of a pole singularity and $\kappa(q,p)$ is the linear susceptibility, p being the Laplace variable.

$$\kappa(q,p) = \sum_k \frac{I_k(q)\Gamma_k(q)}{p + \Gamma_k(q)} \qquad (5)$$

In the well-disordered regime far from the ODT and at low polydispersity, the two modes ($k = 1$ and $k = 2$) are identified with chain self-diffusion (eq 3) and chain relaxation (eq 1) as shown by the theoretical intensities and rates by the dashed lines in Figure 1 for the proximity parameter $\epsilon = 0.55$ and the polydispersity parameter $\langle \delta f^2\rangle = 0.2$. The proximity to ODT measured by the parameter $\epsilon \equiv (\chi^*_{ODT} - \chi^*)/\chi^*_{ODT}$ (from scaling predictions[13,14] the effective segment−segment interaction parameter $\chi^* = \chi\phi^{1.59}$ where χ is the segment−segment interaction parameter in melt) enhances the unfavorable interactions and the susceptibility, $\kappa(q,t)$, according to the dynamic RPA (eqs 4 and 5). Closer to the ODT ($\epsilon = 0.22$) it is the first (slow) mode that is significantly enhanced and hence matches the contribution of the second (fast) process in the q^* region. On the contrary, the amplitude of the fast mode (2) remains

Table 1. Sample Characteristics of High Molecular Mass Styrene-*b*-isoprene (SI) and Styrene-*b*-ethyl propylene (SEP)[a] Diblocks

sample	$M_w \times 10^{-6}$ (LALLS)[b]	f_{PS} (NMR)[c]	M_w/M_n (SEC)[d]	ϕ_{ODT}[e]	q^* (nm^{-1})[e]	ϕ_x
SI2M80	1.60	0.85	1.15	0.079	0.0282	0.055[g]/0.040[f]
(SEP80)				0.061	0.0249	0.035[g]
SI50	0.95	0.52	1.06	0.077	>0.035	0.065[f]
(SEP50)				0.047	0.035	
SI2M20	1.93	0.26	1.09	0.065	0.0306	0.044[g]/0.036[f]
(SEP20)				0.044	0.0154	0.034[f]
SI4M50	3.6	0.49	1.1	0.037	0.018	0.024[g]

[a] ~75% conversion for all SEP samples. [b] THF at 25 °C. [c] $CDCl_3$ at 30 °C. [d] THF at 40 °C. [e] In toluene at 20 °C. [f] Dynamic measurements. [g] Static measurements.

virtually unchanged (cf. Figure 1) and close to that far away from ODT ($\epsilon = 0.55$) in the disordered state. This predicted intriguing dynamic crossover approaching the ODT (at $\epsilon = 0.22$) is experimentally addressed in section IV B.

Finally, it is noted that the intensity $I_2(q)$ (Figure 1) of the second (faster) mode develops two maxima in the vicinity of q^* with increasing proximity ($\epsilon = 0.22$) to ODT. The position of the maxima does not imply the presence of additional characteristic spacing in the system. Instead, they result from the change of the nature of the fast process near the relevant q^* due to the eigenvalue repulsion ($\Gamma_1(q) < \Gamma_2(q)$, ref 9) near the maxima positions of $I_2(q)$.

III. Experimental Section

A. Polymer synthesis. The high molecular weight SI diblocks were synthesized by high vacuum anionic polymerization techniques[17] as described elsewhere.[5,6,9] Styrene was polymerized first, in benzene, using *sec*-BuLi as the initiator, followed by addition of isoprene. Since the concentration of the living PSLi is very low [M_n = (g of monomer)/(mol of *sec*-BuLi)] the unavoidable deactivation of PSLi by the tiny amount of impurities accompanying isoprene leads to an appreciable amount of PS homopolymer in the final reaction product. For this reason, three to five solvent/nonsolvent (toluene/methanol) fractionations were carried out, depending on the molecular weight and composition of the block copolymer, for the removal of PS homopolymer and the isolation of pure diblock copolymers. The weight-average molecular weight of the fractionated diblock copolymers was determined by low-angle laser light scattering, LALLS, in THF at 25 °C and the polydispersity index (M_w/M_n) by size exclusion chromatography, SEC, in THF at 40 °C. The average composition of the copolymers was determined by ^{1}H NMR spectroscopy in $CDCl_3$ 30 °C.

The molecular characteristics of the block copolymers are given in Table 1. The concentration ϕ_{ODT} at which the diblock copolymer solutions in toluene undergo the disorder to order transition at 20 °C was estimated by the sudden change in the scattering intensity $I(q^*)$ and the width of the $I(q)$ peak as a function of concentration; at ϕ_{ODT}, these high molecular weight diblock copolymer solutions became colored due to the light diffraction. Figure 2 shows two representative SEC chromatograms. The styrene-*b*-(ethylene-*alt*-propylene), SEP, samples were obtained by hydrogenating the PI block using the Wilkinson catalyst in dilute toluene under hydrogen pressure.[18] A 400:1 molar ratio of double bonds to catalyst was used. Hydrogen pressure was maintained at 100 psi and temperature of the reaction at 100 °C for 2 days. The extent of hydrogenation amounts to ca. 75% for all samples as determined by ^{1}H NMR spectroscopy.[19] There was no change detected with SEC in the molecular characteristics of the sample after hydrogenation.

B. Photon Correlation Spectroscopy (PCS). The intermediate scattering function $C(q,t) = [G(q,t) - 1)/f^*]^{1/2}$ is obtained from the experimental intensity autocorrelation function $G(q,t) = \langle I(q,t)I(q,0)\rangle/\langle I(q)\rangle^2$ (f^* is the instrumental coherence factor) measured by PCS in the polarized geometry under homodyne conditions over a broad time range (10^{-7}–10^2 s). The scattering wave vector $q = (4\pi n/\lambda)\sin(\theta/2)$ (λ is the laser wavelength in a vacuum, n is the solvent refractive index, and θ is the scattering angle) ranges from 3×10^{-3} to 3.5×10^{-2} nm^{-1}. An ALV-5000 full digital correlator was employed in conjunction with a Nd:YAG laser at $\lambda = 532$ nm. All measurements were carried out at 20 °C. The analysis of the intermediate scattering function $C(q,t)$ ($\propto S(q,t)$) proceeds via inverse, Laplace transformation (ILT):

$$C(q,t) = \int L(\ln \tau)\exp(-t/\tau)d(\ln \tau) \qquad (6)$$

In the present case, no assumption is made for the shape of the distribution of relaxation times, $L(\ln \tau)$, except that $C(q,t)$ is a sum of exponentials. The non-single-exponential shape of $C(q,t)$ is clearly revealed by the ILT leading to a non unimodal distribution of the relaxation function $L(\ln \tau)$. The position and the area of each peak in $L(\ln \tau)$ defines the rate, Γ_k, and intensity, $I_k = \alpha_k(q)I(q)$, of the kth process ($k = 1, 2, \ldots$), where

$$\alpha_k(q) = \frac{\int L_k(\ln \tau)\, d(\ln \tau)}{\int L(\ln \tau)\, d(\ln \tau)} \qquad (7)$$

is the fraction of $L(\ln \tau)$ associated with the kth process and $I(q)$ is the total intensity normalized to the polarized intensity of the solvent toluene. For the solutions with concentrations near ODT, the intensity of the incident laser beam was sufficiently low to avoid optical trapping.[20]

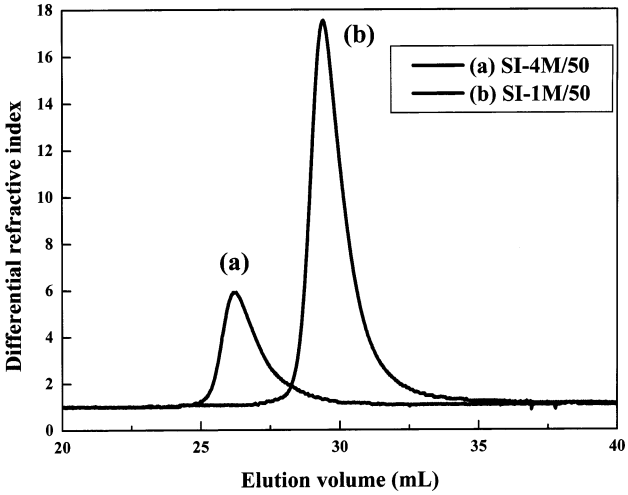

Figure 2. Size exclusion chromatography of (a) SI4M50 and (b) SI50 in THF at 40 °C.

IV. Results and Discussion

A. Static Structure Factor. The development of the characteristic diblock copolymer peak of the static structure factor, $S(q) \propto I(q)/\phi$, at q^* with increasing concentration for SI4M50 in toluene at 20 °C is shown in Figure 3. With increasing polymer concentration, $S(q)$ narrows, its peak intensity, $S(q^*)$, increases, and the

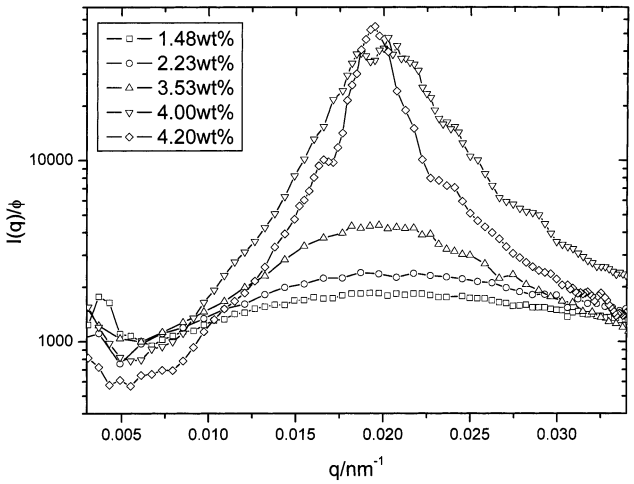

Figure 3. Light-scattering intensity distribution $I(q)/\phi$ for disordered solutions of SI4M50 in toluene at five different block copolymer concentrations (in wt %) at 20 °C.

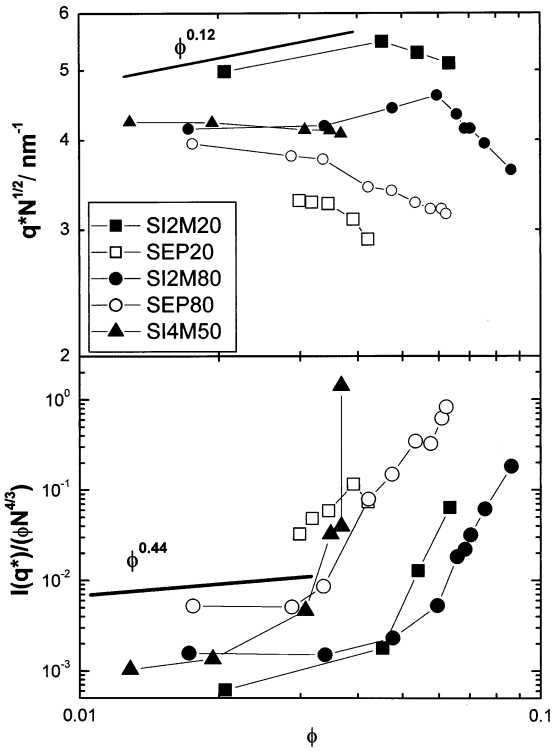

Figure 4. Concentration dependence, ϕ, of the normalized peak position, $q^*N^{1/2}$, and peak intensity, $I(q^*)/(\phi N^{4/3})$, for five different diblock copolymer samples in toluene at 20 °C. The solid lines indicate the scaling predictions of eq 8.

spacing of the structure becomes somewhat larger; i.e., q^* slightly decreases with increasing ϕ. In the other diblock copolymers, this decrease is stronger (Figure 4 below). While the variation of these structural parameters with temperature is well documented for copolymer melts,[8] the effect of concentration under isothermal conditions is experimentally unexplored.[21] On the theoretical side, the concentration dependence of q^* and $I(q^*)/\phi$ has been known for diblock copolymers in good, non selective, solvents.[13,14,22] If we take into account the excluded-volume interactions and composition fluctuations, these relations read as follows:

$$q^* \propto \phi^{0.12} N^{-1/2} \quad I(q^*)/(N\phi) \propto \phi^{0.44} N^{1/3} \qquad (8)$$

To investigate the validity of these scaling predictions, we plot $q^*N^{1/2}$ and $I(q^*)/(N^{4/3}\phi)$ vs ϕ in Figure 4 for the investigated block copolymers with q^* falling inside the light-scattering q window. It can be noted, that up to a certain concentration, ϕ_x, for a given sample (Table 1), the scaling expressions in eq 8 qualitatively capture the weak concentration dependence for both the peak position q^* (Figure 4a) and the peak intensity $I(q^*)$ (Figure 4b). Exceeding this concentration, ϕ_x, in the disordered regime, eq 8 is at odd with the experimental q^* and $I(q^*)$. The observed decrease in q^* resembles the dependence of q^* in block copolymer melts[8] with decreasing temperature ascribed to the chain stretching. A similar effect has also been reported for ordered block copolymer solutions in a neutral−good solvent where q^* increases with dilution due to screening of the unfavorable interaction.[23] In view of eq 8, the strong increase of $I(q^*)/\phi$ above ϕ_x signals the onset of stronger composition fluctuations.

In diblock copolymer melts with $\chi \sim 1/T$, the ODT is approached by decreasing temperature and hence the deviation of $1/I(q^*)$ from the linear $1/T$ dependence, below a certain temperature T_x, is usually taken (see for example ref 8) as an indication of the importance of composition fluctuations corrections. In diblock copolymer solutions in a common solvent, the analogue plot of $\phi/I(q^*)$ vs ϕ (see for example Figure 1 in ref 7) shows also deviation from a linear ϕ dependence above some concentration ϕ_x. It indicates that the diblock copolymer solutions are more compatible than anticipated from the mean-field theory in analogy to the AB block copolymer melts below T_x. Hence, these conformational and fluctuation effects, due to changes in the local composition field near T_x and ϕ_x, indicate similar real space morphologies in the melt and in solution at comparable ϵ values.

B. Dynamic Structure Factor. To examine the predicted dynamic crossover of the dominant process in $S(q \sim q^*,t)$ (Figure 1) approaching the ODT, we utilize the most monodisperse sample, SI50. At low concentrations far below ϕ_x, the dominant process of $S(q,t)$ is the overall chain relaxation, Γ_2 (eqs 4), whereas the self-diffusive mode with the q^2-dependent rate, $\Gamma_1 = q^2D_s$, was resolved at low q's (see ref 7 for 2.85 wt %). Approaching ϕ_x, the main process of the intermediate scattering function, $C(q,t)$, continues to be insensitive to the change of the wave vector, **q** (as it was at $\phi \ll \phi_x$, ref 7), indicated by the similarity between the $C(q,t)$ of 5.25 wt % SI50 toluene solution at three different q's in the upper part of Figure 5; note that if diffusive dynamics were dominant, the $C(q,t)$ at $q = 0.0135$ nm^{-1} would be by about one decade slower than that at the highest q. The insensitivity of the main process to q-variations is also revealed by the inverse Laplace transformation (eq 6) of the intermediate scattering functions shown in the lower plots of Figure 5. The main peak (2) of the distribution $L(\ln \tau)$ occurring at the same time irrespectively of the magnitude of the wave vector relates to the overall chain relaxation, Γ_2. At the two lower wave vectors, a second slower peak (1) can be resolved in the $L(\ln \tau)$. This peak shifts to longer times with decreasing q, conforming to a diffusive behavior. The broader shape of $C(q,t)$ at the lowest q in Figure 5 reflects the decreasing contribution of the fast mode (2) and its increasing separation in time scale from the diffusive mode (1). The fast process in Figure 5 is easily identified as the cooperative diffusion because of its diffusive rate and its q-independent intensity as ex-

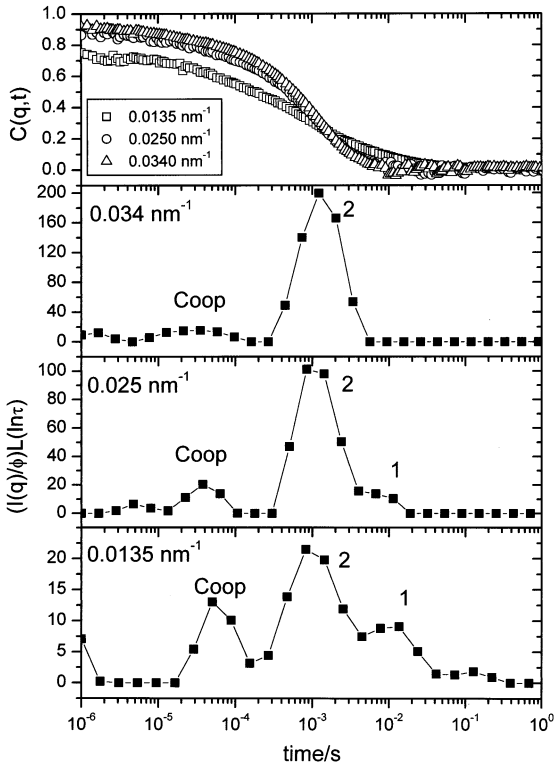

Figure 5. Intermediate scattering function $C(q,t)$ (upper part) at three different wave vectors for 5.25 wt % SI50 in toluene at 20 °C along with the reduced distribution of relaxation times $(I(q)/\phi)L(\ln \tau)$ (eq 6) with $I(q)$ being the total light-scattering intensity. The peaks in $L(\ln \tau)$ associated with the cooperative diffusion and the relaxation modes 1 and 2 are indicated in the plot.

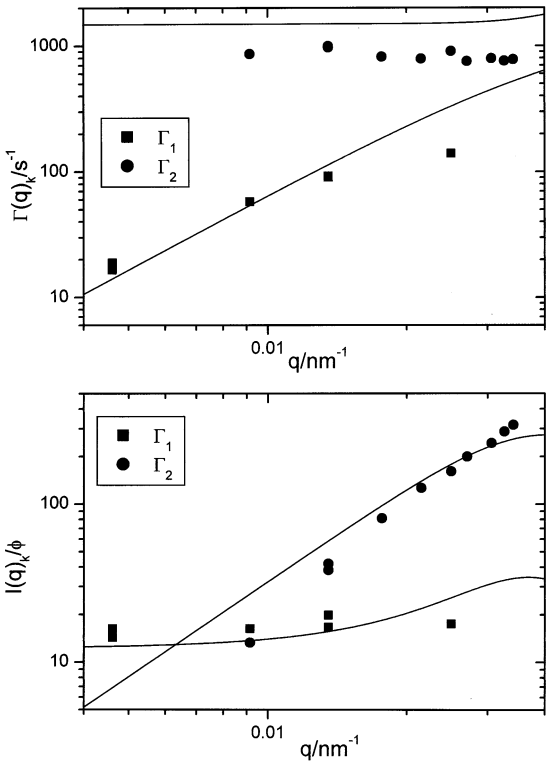

Figure 6. Experimental (symbols) and theoretical (eqs 4 and 5) (lines) relaxation rates, Γ_k, and intensities, I_k, of the two main processes ($k = 1,2$) associated with the order parameter fluctuations in 5.25 wt % SI50 in toluene at 20 °C.

pected for the relaxation of short-range total concentration fluctuations in semidilute homopolymer solutions;[10] this mode is not diblock copolymer specific.[3,6] Thus, the ILT analysis (eq 6) yields a consistent and physically meaningful representation of the experimental $C(q,t)$ near the ODT.

Next, the q dependence of the relaxation rates, Γ_k, and the reduced intensities, $I_k(q)/\phi$ ($k = 1,2$), are displayed in Figure 6. The upper part clearly demonstrates the q-independence of Γ_2 and the q^2 dependence of Γ_1. The corresponding reduced intensities, $I_k(q)/\phi$, of the two processes show that the pure relaxational mode (2) is the dominant process since it captures the peak of $S(q)$ at a finite $q^* > 0.035$ nm^{-1}. A very similar picture for the static and dynamic structure factor was displayed by the SI50 sample at lower concentrations (2.85 wt % Figure 6a in ref 7) in agreement with the theoretical predictions of eqs 4 and 5 with a radius of gyration $R_g = 50$ nm, $\Gamma_0 = 1/\tau_0 = 2500$ s^{-1}, composition polydispersity $\langle \delta f^2 \rangle = 0.2$ and proximity to the ODT $\epsilon = 1 - (\phi/\phi_{ODT})^{1.59} = 0.8$.

To compare the predictions of eqs 4 and 5 with the data of Figure 6 for the same SI50 but at the higher concentration of 5.25 wt %, the parameters ϵ and Γ_0 should be readjusted because of the closer proximity to ϕ_{ODT} and the lower mobility compared with the lower (2.85 wt %) concentration. An agreement between the experimental data (symbols) and the theoretical (lines) values of the rates, Γ_k, and the intensities, I_k, was obtained using the following values: $R_g = 50$ nm, $\Gamma_0 = 1500$ s^{-1}, $\langle \delta f^2 \rangle = 0.2$, and $\epsilon = 0.55$ ($\phi_{ODT} = 0.077$). To match the theoretical to the experimental intensities we used a concentration independent intensity parameter, A, proportional to the optical contrast between the two blocks. Thus, A, R_g, and $\langle \delta f^2 \rangle$ are system specific parameters independent of concentration and are therefore kept fixed for all theoretical fits to the data of a given block copolymer system. Overall, the simultaneous representation of the partial intensities (I_1, I_2) and the rates (Γ_1, Γ_2) by eqs 4 and 5 is adequate. However, the theoretical description of the two rates is less satisfactory. In the theory the ratio $\Gamma_2/(\Gamma_1/q^2)$ at low q's is independent of concentration and this assumption is probably the reason for incomplete theoretical representation of the two experimental rates simultaneously. Experimentally, $D_s = \Gamma_1/q^2$ (at low q's) decreases by 50% whereas Γ_2 slows down by 40% between 2.85 and 5.25 wt %.

When the concentration is increased further, beyond ϕ_x, we clearly observe a change of the nature of the dominant process of $S(q \sim q^*,t)$. From the $C(q,t)$ of 8.46 wt % SI50 in toluene at 20 °C (upper part of Figure 7) and the corresponding distributions $(I(q)/\phi)L(\ln \tau)$, we observe that the slow process (1) now dominates the $S(q,t)$; the observed extra slow mode at high q values is an artifact due to baseline fluctuations. The use of the normalized $(I(q)/\phi)L(\ln \tau)$ distribution allows for a comparison between different concentrations as seen, for example, in Figures 5 and 7. The fast process (2), dominant at $\phi < \phi_x$ (Figure 5), can now be resolved only at lower q's and is distinguished by its q-independent rate.

On the basis of the variation of the relaxation rates, Γ_k, and the reduced intensities, $I_k(q)/\phi$ with q (Figure 8) the dominant process of $S(q,t)$ clearly bears the characteristics of the diffusive process (1). Its intensity, $I_1(q)/\phi$ is q-independent at low q's but increases with q above about 0.015 nm^{-1} and peaks at a finite $q^* > 0.035$ nm^{-1}; the $I_1(q \sim q^*)/\phi$ at 8.46 wt % is much higher than

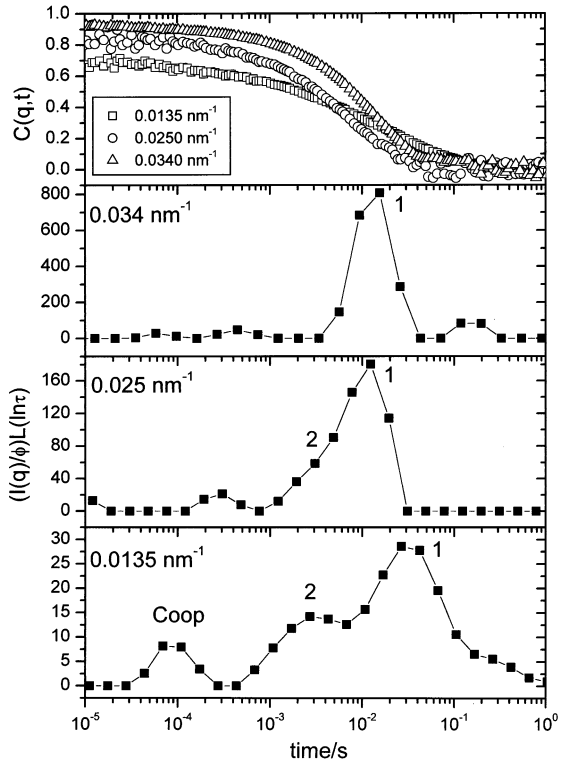

Figure 7. Intermediate scattering function $C(q,t)$ (upper part) at three different wave vectors for 8.46 wt % SI50 in toluene at 20 °C along with the reduced distribution of relaxation times $(I(q)/\phi)L(\ln \tau)$ (eq 6) with $I(q)$ being the total light-scattering intensity. The peaks in $L(\ln \tau)$ associated with the cooperative diffusion and the relaxation modes 1 and 2 are indicated in the plot.

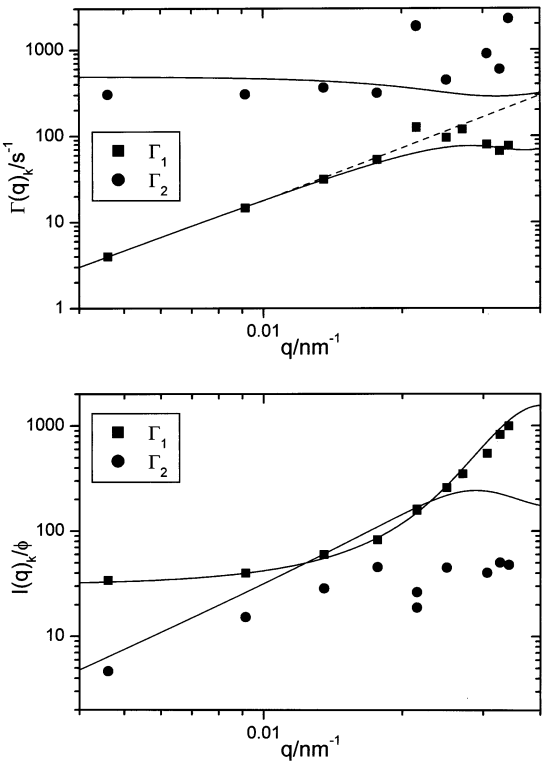

Figure 8. Experimental (symbols) and theoretical (eqs 4 and 5) (lines) relaxation rates, Γ_k, and intensities, I_k, of the two main processes ($k = 1, 2$) associated with the order parameter fluctuations in 8.46 wt % SI50 in toluene at 20 °C. The dashed line indicates the diffusive (q^2 dependence) nature of Γ_1 at low q's extrapolated to high q's.

at 5.25 wt % in Figure 6. If mode (2) were responsible for $S(q^*)$ as it was the case in Figure 6, then Γ_1 would have assumed an unreasonably strong q dependence. Besides, $I_1(q \sim q^*)/\phi$ was found to systematically increase with concentration above about 6 wt % and become comparable to $I_2(q \sim q^*)/\phi$ at about 7.2 wt % ($\sim\phi_x$).

On the theoretical side, this mode assignment is favored by eqs 4 and 5. The comparison with the theoretical model of section II.B can proceed with the same fixed parameters (R_g, $\langle \delta f^2 \rangle$, A) changing $\epsilon = 0.1$ (closer proximity to the ODT) and $\Gamma_0 = 500\ s^{-1}$ (reduced mobility due to the higher block copolymer concentration). Both characteristics (rate $\Gamma_1(q)$ and intensity $I_1(q)$) of the "new" main process are well captured by the model predictions (lines in Figure 8) also above this dynamic crossover concentration ($\sim\phi_x$). Note also that the large increase of $I_1(q \sim q^*)$ leads to a reduction of Γ_1 relative to its diffusive value (dashed line in Figure 8) close to q^*. This "thermodynamic" slowing down effect (ref 9 and Figure 9b, below) is well captured by the theory (eqs 4 and 5). The theory, however seems to overestimate the intensity $I_2(q)$ which is not affected by the increasing proximity to the ODT (cf. Figures 6 and 8). The observed disparity with the experimental $I_2(q)$ is beyond the large error involved in the determination of $I_2(q)$ near q^*. A related observation was reported[7] for the hydrogenated counterpart of SI50.

At higher molecular weights, which are desired to shift q^* well within the light-scattering q-window, the polydispersity is bound to be larger, and hence, the diffusive mode (1) becomes dominant even at low concentrations. For the SI4M50 sample at 1.48 wt % in toluene at 20 °C, the diffusive mode (1) is indeed the dominant process (Figure 9, left part), but the polydispersity is sufficiently low to allow for the resolution of the fast process (2) as well. Hence, the dynamic response of this sample is between that of SI50 and SI2M (of ref 9 that displayed only the diffusive process (1)) and offers an intermediate case to contrast with the theoretical predictions. A good agreement between experiment and theory was found in Figure 9 using the values for the fitting parameters: $R_g = 100$ nm, $\Gamma_0 = 1000\ s^{-1}$, $\langle \delta f^2 \rangle = 0.67$, and $\epsilon = 0.36$. This ϵ value is too low compared to the estimated $\epsilon = 0.81$ from the experimental $\phi_{ODT} = 0.037$. It is worth mentioning that a too low ϵ was required to represent $S(q,t)$ of the polydisperse SEP50 of ref 7 as well. It appears that the theoretical description of $S(q,t)$ of moderately polydisperse diblock copolymers well in the disordered regime underestimates ϕ_{ODT}.

At concentrations close to the ODT, for example 4.00 wt % SI4M50 in toluene at 20 °C, the diffusive mode (1) remains the dominant process of $S(q,t)$ and exhibits a pronounced slow of Γ_1 at q^* as depicted in the right part of Figure 9. The second faster mode (2) can be resolved in the q range where the intensity of the diffusive process is not too high, i.e., away from q^*. The theory is in a good agreement with the experimental data using the same fixed parameters as for the lower concentration but $\Gamma_0 = 50\ s^{-1}$ and $\epsilon = 0.01$. The huge increase of the total $S(q^*)$ for the 4.00 wt % as compared to the 1.48 wt % solution in Figure 3 is exclusively caused by the intensity $I_1(q^*)$ of the slow mode (1) (Figure 9), while the intensity $I_2(q^*)$ is insensitive to the proximity to the ODT. The model captures well all experimental features for both processes including the slowing down of Γ_1 at q^*. However, the value of the

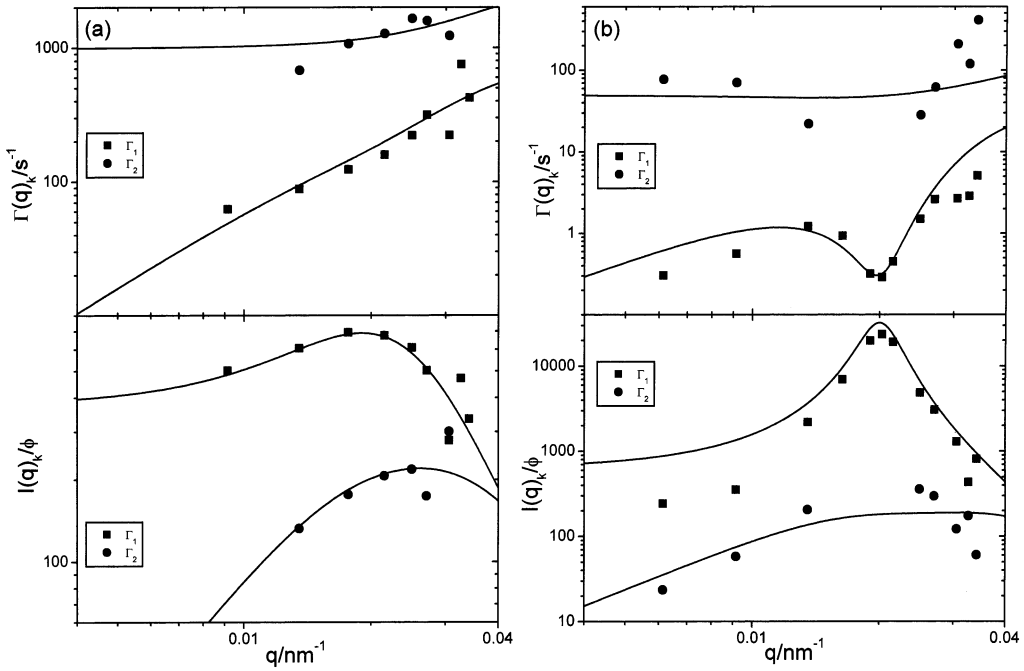

Figure 9. Experimental (symbols) and theoretical (eqs 4 and 5) (lines) relaxation rates, Γ_k, and intensities, I_k, of the two main processes ($k = 1, 2$) associated with the order parameter fluctuations in (a) 1.48 wt % (left) and (b) 4.00 wt % (right) SI4M50 in toluene at 20 °C.

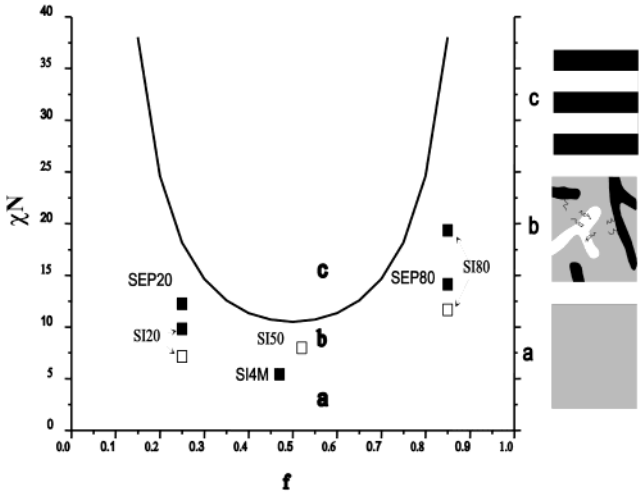

Figure 10. Mapping of the experimental crossover concentrations ϕ_x of the different SI and SEP system on the mean-field phase diagram of diblock copolymers in a nonselective good solvent. Solid and points indicate the estimated values of ϕ_x from static and dynamic structure factor, respectively. Insets a−c sketch the real space morphology of AB diblock copolymers in the disordered state, fluctuation regime, and ordered state, respectively.

adjustable parameter ϵ is again lower than the expected value from experimental ϕ_{ODT} i.e., the theoretical description requires lower ϕ_{ODT}.

C. Phase Diagram. The mean-field phase behavior of diblock copolymer melts has been extensively investigated both theoretically and experimentally. In Figure 10, we project our static and dynamic data onto the phase diagram of copolymer solutions in a good nonselective solvent.[13,14] The estimation of χN for the different copolymer concentrations is based on the scaling prediction

$$\chi N = (\chi N)_{ODT}\left(\frac{\phi}{\phi_{ODT}}\right)^{1.59} \qquad (9)$$

and the mean field value $(\chi N)_{ODT}$ at the ODT. The concentrations, ϕ_x, at which the deviations from the mean-field predictions (eq 8) occur are indicated in Figure 10 (solid points) along with the dynamic crossover for SI50, SI2M80, and SI2M20 (open points). Below ϕ_x the system is homogeneous and disordered (inset a). At a critical χN corresponding to ϕ_x the interactions become strong enough to create short-lived microdomains rich in block A or B, creating microscopic inhomogeneities in the disordered phase. This is evident from the abrupt increase of the total $I(q^*)$ in Figure 4. Because of these composition fluctuations, the characteristic distance of the system increases i.e., q^* decreases[23] (Figure 4). The behavior resembles the situation in the bulk diblock copolymers where the ODT is approached by decreasing temperature.

Changes in the real state morphology in Figure 10 are also manifested in the $S(q,t)$ observed as the dynamic crossover in the SI50, SI2M80, and SI2M20 systems at $\phi \approx \phi_x$. From the two relevant relaxation mechanisms in $S(q,t)$, it is the slow collective chain diffusion that becomes the effective channel to relax the order parameter fluctuations sketched in inset b. Remarkably the contribution of the relaxational fast mode (2) to $S(q,t)$ is insensitive to ϕ_x. The non-mean-field picture (b) can be produced by superposition of wave position with different amplitudes and q's (not only q^*). The present study shows that their thermal decay predominantly occurs via the collective diffusion (mode 1). Further, beyond this ϕ range D_s undergoes stronger ϕ dependence than expected for entangled homopolymers (see section below).

The hydrogenation of the I-block provides a way to enhance the composition polydispersity at constant M_w/M_n as discussed for the well disordered state elsewhere.[7] Concurrently, the chemical transformation of the I-block also enhances the incompatibility between the two blocks in the SEP copolymers. This is directly reflected in the lower ϕ_{ODT} values of the SEP/toluene than precursor SI/toluene solutions (Table 1). Moreover, the

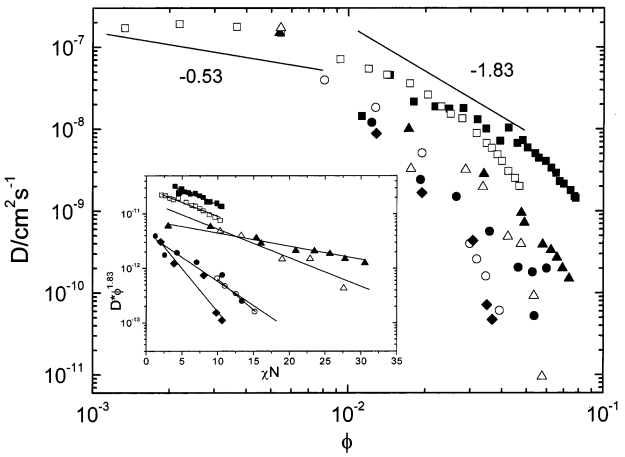

Figure 11. Chain self-diffusion coefficient (D_s) as a function of diblock concentration ϕ: SI50 (■), SEP50 (□), SI80 (●), SEP80 (○), SI20 (▲), SEP20 (△), and SI4M50 (◆) The solid lines indicate the scaling predictions for unentangled and entangled polymer solutions. Inset: $D_s\phi^{1.83}$ vs χN plot for all examined disordered solutions along with the fit of eq 10 (solid lines).

assumption of an impartial behavior of the toluene solvent for the two blocks in SEP is probably not valid very near ODT.

D. Self-Diffusion. At low q's the diffusive process (1) has been identified with the self-diffusion of copolymer chains.[3,7] The concentration dependence of the self-diffusion coefficient, D_s extracted from the $S(q,t)$ at low q's, for seven different diblock copolymers is depicted in Figure 11; the contribution $2\kappa_0\chi N\phi^{1.59}$ in the expression of Γ_p in eq 3 is much less than one. At low concentrations, in the unentangled solutions, D_s changes slowly with concentration while in the entangled solutions the rate of decrease of D_s increases. In the two concentration regimes, D_s should theoretically follow the Rouse ($\phi^{-0.53}$) and the reptation scaling ($\phi^{-1.83}$); the latter was found to represent D_s in low molecular mass diblock copolymers.[24] With further increase of the concentration, beyond about ϕ_x, toward the ODT an even stronger decrease of D_s is observed for all examined diblock copolymer solutions.

Evidence of retardation of the self-diffusion in the disordered state near the ODT was reported for entangled diblock copolymer melts studied by forced Rayleigh scattering.[25] On the theoretical side, D_s is predicted[26] to become slower than the classical Rouse near the ODT. More recently, computer simulations[12] of both symmetric and asymmetric diblock copolymer melts have suggested the utility of the purely thermodynamically suppression, $D_s \sim \chi N^a f(1-f)$, where the exponent a assumes values between 0.5 and 1. The experimental diffusion data of Figure 11, treated as $D_s\phi^{1.83}$ near ODT, do not conform to this proposed scaling.

Lodge and Dalvi[27] have suggested that the self-diffusion in ordered lamellar diblock copolymer melts is retarded due to thermodynamic and entanglement constrains. The retardation followed a single exponential relation with χN

$$D_s = D_0 \exp(-\alpha\chi N) \qquad (10)$$

with an activation barrier α. It is noteworthy to mention that Rah and Eu[28] derived an analogue expression for the diffusion coefficient of a molecular liquid, $D = D_0 \exp(-W/k_BT)$ where W represents the work needed to create a characteristic space that is necessary for the particle diffusion. Since $\chi N \propto 1/k_BT$ and α can be identified with W, eq 10 is recovered. The apparent insensitivity of D_s to the ODT allows us to employ this equation in the disordered regime beyond the ODT as well.

To describe the retardation of D_s approaching the ODT in the present diblock copolymer solutions by eq 10, we plot $D_s\phi^{1.83}$ vs χN as shown in the inset of Figure 11; χN was estimated by using eq 9 for all concentrations above ϕ_x. In this plot, the decrease of D_s with χN should be caused by the activation barrier α. Indeed the single exponential dependence of eq 10 can represent the data with α ranging from 0.05 to 0.4 that should be compared with $\alpha = 0.24$ in the diblock copolymer melt.[27] Given the errors involved in the transformation of the main plot of Figure 11, the hindrance in the center of mass motion due to thermodynamic effects are of the same order in both melt and solution of diblock copolymers. Moreover, the extent of the retardation exerted by the composition fluctuations on D_s appears to be molecular weight dependent. For the seven diblock copolymer systems of Figure 11, a systematically increase of α, from the lowest (SI50) to the highest (SI4M50) molecular mass sample (Table 1), can be parametrized as $\alpha \propto M$. This dependence probably reflects the extent of entanglements that seems to be the prerequisite[25] for the thermodynamic slowing down of D_s.

E. Concluding Remarks. Three main new messages emerge from the present static and dynamic study of diblock copolymer solutions in a common solvent near the ODT.

(i) The shape of the dynamic structure factor $S(q,t)$ can predominantly be either diffusive or pure relaxational-like depending on the composition polydispersity[7] and the real space morphology as given in the phase diagram of diblock copolymers.[8,13] Above about $\phi_x < \phi_{ODT}$, where composition fluctuation corrections become important for the static $S(q)$, $S(q,t)$ displays a dynamic crossover for its main relaxation process. Including composition polydispersity, the theory predicts surprisingly well this behavior of $S(q,t)$.

(ii) The chain self-diffusivity D_s obtained from the $S(q,t)$ at low qR values undergoes a thermodynamic slowing down above ϕ_x which depends on their total molar mass.

(iii) The predicted[13,22] weak concentration dependence of $S(q^*)$ and q^* cannot describe these experimental quantities over the whole concentration range up to ϕ_{ODT}; deviations are observed above about ϕ_x. The two previous papers[6,7] (part 1 and part 2) and the present study complete the experimental investigation of $S(q,t)$ of diblock copolymer solutions over a broad time range, wave vectors q on both side of q^* and different compositions, symmetric and asymmetric once.

Summing up, the dynamic response of this important class of materials in the disordered regime from far away to very close to the ODT can be controlled experimentally by proper sample design.

Acknowledgment. The financial support of the EU (Grant FMRX-CT 97-0112) is gratefully acknowledged.

References and Notes

(1) Benmouna, M.; Benoit, H.; Borsali, R.; Duval, M. *Macromolecules* **1987**, *20*, 2620.

(2) Duval, M.; Picot, C.; Benoit, H.; Borsali, R.; Benmouna, M.; Lartigue, C. *Macromolecules* **1991**, *24*, 3185.
(3) Jian, T.; Anastasiadis, S. H.; Semenov, A. N.; Fytas, G.; Adachi, K.; Kotaka, T. *Macromolecules* **1994**, *27*, 4762.
(4) Pan, C.; Lodge, T. P.; Stepanek, P.; von Meerwall, E. D.; Watanabe, H. *Macromolecules* **1995**, *28*, 1643.
(5) Semenov, A. N.; Anastasiadis, S. H.; Boudenne, N.; Fytas, G.; Xenidou, M.; Hadjichristidis, N. *Macromolecules* **1997**, *30*, 6280.
(6) Sigel, R.; Pispas, S.; Hadjichristidis, N.; Vlassopoulos, D.; Fytas, G. *Macromolecules* **1999**, *32*, 8447.
(7) Holmqvist, P.; Pispas, S.; Hadjichristidis, N.; Fytas, G. *Macromolecules* **2002**, *35*, 3157.
(8) Rosedale, J. H.; Bates, F. S.; Almdal, K.; Mortensen, K.; Wignall, G. D. *Macromolecules* **1995**, *28*, 1429.
(9) Chrissopoulou, K.; Pryamitsyn, V. A.; Anastasiadis, S. H.; Fytas, G.; Semenov, A. N.; Xenidou, M.; Hadjichristidis, N. *Macromolecules* **2001**, *34*, 2156.
(10) De Gennes, P. G. *Scaling concept in Polymer Physics*; Cornell University Press: Ithaca, NY, 1979.
(11) Doi, M.; Edwards, S. F. *The Theory of Polymer Dynamics*; Oxford Science Publishers: Oxford, England, 1986.
(12) Hoffmann, A.; Sommer, J. U.; Blumen, A. *J. Chem. Phys.* **1997**, *107*, 7559.
(13) Fredrickson, G. H.; Leibler, L. *Macromolecules* **1989**, *22*, 1238.
(14) Whitmore, M. D.; Noolandi, J. *J. Chem. Phys.* **1990**, *93*, 2946.
(15) Erukhimovich, I. Y.; Semenov, A. N. *Sov. Phys. JETP* **1986**, *28*, 149.
(16) Ackasu, A. Z.; Benmouna, M.; Benoit, H. *Polymer* **1986**, *27*, 1935.
(17) Hadjichristidis, N.; Iatrou, H.; Pispas, S.; Pitsikalis, M. *J. Polym. Sci., Part A: Polym. Chem.* **2000**, *38*, 3211.
(18) Mohammadi, N. A.; Rempel, G. L. *J. Mol. Catal.* **1989**, *50*, 259.
(19) Barth, H. G.; Mays, J. *Modern Methods of Polymer Characterization*; Wiley & Sons: New York, 1991.
(20) Sigel, R.; Fytas, G.; Vainos, N.; Pispas, S.; Hadjichristidis, N. *Science* **2002**, *297*, 67.
(21) Lodge, T. P.; Pudil, B.; Hanley, K. J. *Macromolecules* **2002**, *35*, 4707.
(22) Olvera de la Cruz, M. *J. Chem. Phys.* **1989**, *90*, 1995.
(23) Lai, C.; Russel, W. B.; Register, R. A. *Macromolecules* **2002**, *35*, 4044.
(24) Anastasiadis, S. H.; Chrissopoulou, K.; Fytas, G.; Appel, M.; Fleischer, G.; Adachi, K.; Gallot, Y. *Acta Polym.* **1996**, *47*, 250.
(25) Dalvi, M. C.; Eastman, C. E.; Lodge, T. P. *Phys. Rev. Lett.* **1993**, *71*, 2591.
(26) Genz, U.; Vilgis, T. A. *J. Chem. Phys.* **1994**, *101*, 7111.
(27) Lodge, T. P.; Dalvi, M. C. *Phys. Rev. Lett.* **1995**, *75*, 657.
(28) Rha, K.; Eu, C. B. *Phys. Rev. Lett.* **2002**, *88*, 65901.

MA021402P